AIP | Conference Proceedings

Solar energetic particles: Shock acceleration and transport through self-amplified waves

Chee K. Ng, Donald V. Reames, and Allan J. Tylka

Citation: AIP Conf. Proc. **1436**, 212 (2012); doi: 10.1063/1.4723610
View online: http://dx.doi.org/10.1063/1.4723610
View Table of Contents: http://proceedings.aip.org/dbt/dbt.jsp?KEY=APCPCS&Volume=1436&Issue=1
Published by the American Institute of Physics.

Solar Energetic Particles: Shock Acceleration and Transport through Self-Amplified Waves

Chee K. Ng[*,†], Donald V. Reames[**] and Allan J. Tylka[†]

[*]George Mason University, Fairfax, VA, USA
[†]Naval Research Laboratory, Washington DC, USA
[**]University of Maryland, College Park, MD, USA

Abstract. This article reviews our work on the powerful influence of self-amplified Alfvén waves on the interplanetary (IP) transport and shock acceleration of solar energetic particles (SEPs). In large gradual events, a huge number of shock-accelerated protons stream through the IP medium and amplify ambient Alfvén waves by orders of magnitude. Nonlinear models that take account of self-amplified waves semi-quantitatively explain many intriguing SEP observations at 1 AU: (a) upper limits to early SEP intensities, (b) flat intensity energy spectra up to $\sim$ 30 MeV/amu before shock arrival, and (c) complex temporal, energy, and event-to-event variations of elemental abundances. Streaming limit complicates estimation of the number and energy of SEPs accelerated in a solar event but provides a safety window for astronauts to seek shelter before a potential hazardous intensity rise at shock passage. Self-amplified waves help bootstrap shock acceleration and the high near-shock SEP intensity predicted at $\leq 20\, r_\odot$ is relevant to inner heliospheric space missions.

Keywords: solar energetic particles, coronal shock acceleration, self-excited plasma waves
PACS: 96.50.Vg, 96.50.Fm, 96.50.Tf, 96.50.Pw

INTRODUCTION

Anti-sunward Alfvén waves are greatly amplified by streaming SEPs upstream of a CME-driven coronal shock in a large gradual SEP event. The amplified waves profoundly influence the shock acceleration and transport of all ion species. They throttle ion transport in a rigidity, ion species, and pitch-angle dependent manner, limiting SEP intensity away from the shock and producing complex temporal and event-to-event variations of SEP abundances. Upstream of a quasi-parallel CME-driven coronal shock, Alfvén waves intensely amplified by protons below the 'knee' energy E_{knee} scatter protons and ions of higher rigidities at larger pitch-angles, bootstrapping SEP acceleration.

We can understand many intriguing SEP observations by taking account of the resonant interaction between SEPs and Alfvén waves *self-consistently*. The dominant cyclotron resonance condition $\omega - k\mu v = -\Omega/\gamma$ may be rewritten:

$$\frac{k}{B} = \frac{1}{P(\mu - V_A/v)} = \frac{Q}{A}\frac{1}{\gamma v(\mu - V_A/v)}\frac{e}{m_p c}, \tag{1}$$

where ω is angular wave frequency, k wavenumber, μ pitch-angle cosine, v ion speed, Ω angular cyclotron frequency, γ Lorentz factor, B magnetic field, P rigidity, V_A Alfvén speed, Q ion charge in units of e, A atomic mass, m_p proton mass, and c light speed.

Eq. (1) is key to qualitatively understanding the dependence of SEP characteristics on particle rigidity P (middle term) and mass-to-charge ratio A/Q (last term).

Physics of the Heliosphere: A 10 Year Retrospective
AIP Conf. Proc. 1436, 212-218 (2012); doi: 10.1063/1.4723610

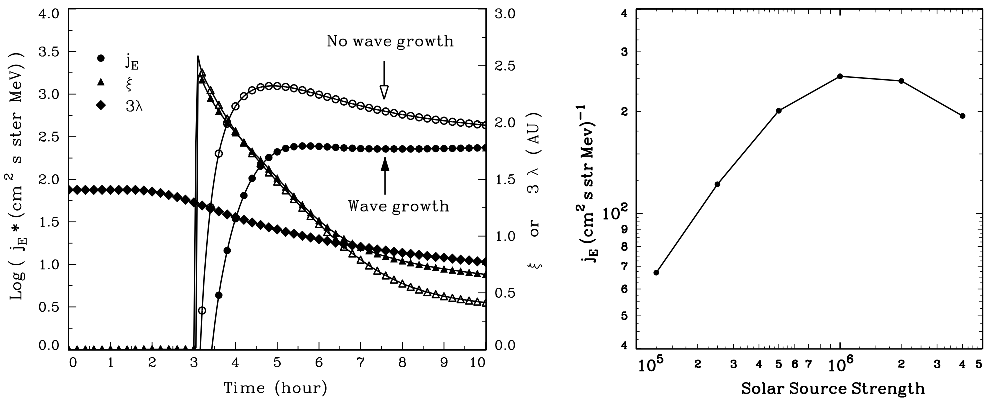

FIGURE 1. (a) Predicted 1 MeV proton intensity j_E, anisotropy ξ, and mean free path λ at 1 AU with/without wave amplification. (b) Peak proton intensity vs SEP source strength (Ng and Reames [1]).

STREAMING LIMITS

The effect of wave amplification on SEP transport was first explored using a time-dependent nonlinear model (Ng and Reames [1]) for a 0.136 - 6.15 MeV, exponentially decaying proton source at a *fixed* radial distance $r_0 = 21r_\odot$. Initially, $I^{R+} = I^{L+}$ intensities of right and left-hand circularly polarized, outward propagating, ambient Alfvén waves are initialized via steady-state solutions to the wave kinetic equation and $I^{R-} = I^{L-} = 0.1\,I^{R+}$ are prescribed for the inward waves.

The Alfvén waves scatter SEPs and self-consistently the SEPs amplify/damp the waves. Focusing in a radial magnetic field is also included. Comparing the predicted 1 MeV proton intensities at 1 AU with/without wave growth, Figure 1a shows that the self-amplified waves greatly reduce the proton intensity j_E. Moreover, the peak j_E increases with source strength to ~ 250 pfu and *decreases* thereafter (Fig. 1b). The intensity reduction is severe for a strong SEP source. Here, pfu $\equiv$ (cm^2 s ster MeV)$^{-1}$ and 'source strength' is the source SEP intensity in pfu at 1 MeV, $r = r_0, t = 0$.

A survey of SEP events (1 Jan 1988 - 1 Sep 1997) found approximate intensity limits of 250, 10, and 1 pfu for 10, 40, and 100 MeV protons (Fig. 2a) (Reames and Ng [2]). *These limits apply well before shock arrival*. The Ng et al. [3] model extends the previous fixed source model [1] to include a moving multi-ion SEP source at a *traveling* shock, solar-wind convection, adiabatic deceleration, and wave transport. Snapshots of its predicted radial profile of 5.2 MeV proton intensity (Fig. 2b) show that at a *fixed* heliocentric distance (e.g., $r = 1$ AU) the intensity is streaming-limited *early* in an event but rises when the shock comes sufficiently close.

Early intensities above the streaming limits found in the above survey have been reported by e.g., Lario et al. [4], who explored possible causes including the effect of large-scale interplanetary (IP) structures. Of course, the streaming limit also depends on IP parameters. In the Ng et al. [3] model, it varies by a factor of a few for a ten-fold decrease in the ambient wave intensity. Interestingly, for a fixed energetic proton phase-space density, the resonant wave growth rate γ evaluated at k/B is independent of B and varies as $1/\sqrt{n_p}$, with n_p the plasma proton number density.

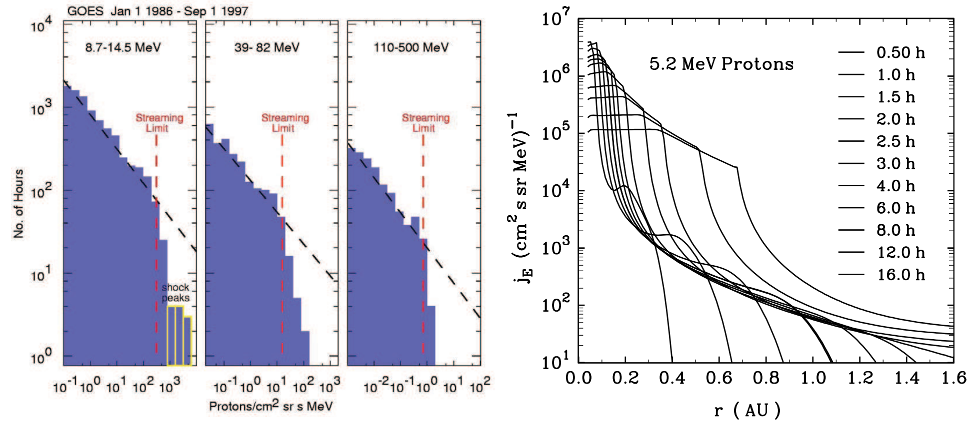

FIGURE 2. (a) Event histogram (1988-1997) vs peak proton intensity and inferred streaming limits for three energies at 1 AU (Reames and Ng [2]). (b) Evolving 5.2 MeV proton j_E vs r profile for a SEP source at a moving shock in a simulation by the Ng et al. [3] model. At r = 1 AU, the intensity is streaming-limited until the shock, located at the sharp knee in each profile, passes 0.5 AU at 12 h.

Streaming limit is implicit in the steady-state shock acceleration models of Bell [5], Lee [6], and Gordon et al. [7] and explicitly studied in a more complex steady-state model of Lee [8]. The result of a multi-parameter study on streaming limit in the time-dependent model and comparison with steady-state models will be reported in [9].

ELEMENTAL ABUNDANCE VARIATION

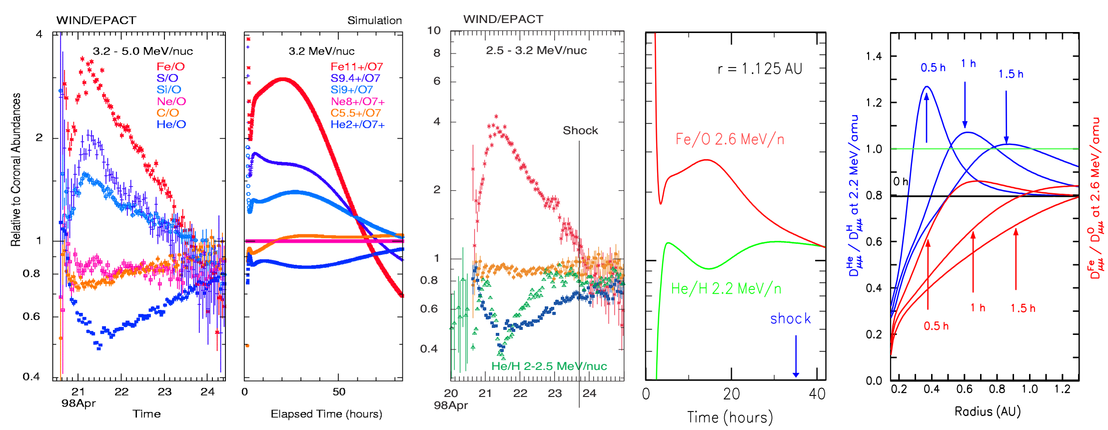

FIGURE 3. (a) Normalized abundance ratios observed in the 1998 April 20 event. (b) Model predicted ratios for indicated charged states. (c) Contrasting observed histories of Fe/O and He/H. (d) Model predicted He/H and Fe/O. (e) Snapshots of the radial profiles of the ratios of $D_{\mu\mu}$ at $\mu = 0.9$ between 2.2 MeV/nuc He^{2+} and H^{+} and between 2.6 MeV/nuc Fe^{14+} and O^{8+}. Arrows give locations of a hypothetical *unscattered* $\mu = 0.9$ ion. (From Tylka et al. [10], Ng et al. [11], Tylka [12]).

The 1998 April 20 event [10, 11, 12] exemplifies the fascinating puzzle of SEP elemental abundance variations. Figure 3a shows Wind/EPACT observation of Fe/O, S/O, Si/O, Ne/O, C/O, and He/O histories at equal energy/amu (i.e. speed). The curves are ordered by A/Q (i.e. rigidity) and show a fall-rise-fall pattern for ratios of high A/Q to low A/Q ions. There is an *intriguing exception* to the rigidity ordering: He/H varies in anti-phase to Fe/O (Fig. 3c). While the initial fall in abundance ratio in Fig. 3a is expected because the μ-diffusion coefficient $D_{\mu\mu}$ is smaller for higher A/Q ions in a Kolmogorov ambient wave spectrum, the ratio rebound and He/H violation of A/Q ordering (Figs. 3a,c) present a twin challenge to SEP transport in a *passive* medium.

By including wave growth and a moving multi-ion source, the Ng et al. [11] model semi-quantitatively produces both the rebound (Fig. 3b) *and* the He/H behavior (Fig. 3d). We can understand this qualitatively via Eq. (1) as follows. Consider X and Y minor ions of equal energy/amu E/A, equal μ, and $A_Y/Q_Y > A_X/Q_X > 1$. Wave growth is dominated by the contribution of energetic protons and the more numerous protons at low-energy amplify Alfvén waves faster at the higher wavenumbers resonant with lower rigidity X. As scattering of X increases relative to Y, the Y/X ratio rebounds (Figs. 3a,b).

Moreover, if ample protons of higher speed vA_Y/Q_Y *run ahead* to amplify waves resonant with Y *but not* X at speed v (Eq. (1)), then the *earliest* Y will be 'anomalously' scattered more than X and Y/X will rise *initially* in apparent violation of A/Q ordering. The 'violation' is observed for 2.2 MeV/amu He^{2+}/H^{+} but not 2.6 MeV/amu Fe^{14+}/O^{8+} in the 1998 April event (Fig. 3c,d). The model reveals that at $\mu = 0.9$, numerous ≥ 9 MeV protons amplify waves to modify $D^{He}_{\mu\mu}/D^{H}_{\mu\mu} = 0.8$ to $D^{He}_{\mu\mu}/D^{H}_{\mu\mu} > 1$ in a moving 'barrier' to early 2.2 MeV/amu He^{2+}. In contrast, $D^{Fe}_{\mu\mu}/D^{O}_{\mu\mu}$ remains < 1 everywhere because there are few ≥ 42 MeV protons running ahead to amplify the required resonant waves for 2.6 MeV/amu Fe^{14+} (Fig. 3e).

If there are ample ≥ 9 MeV protons, 2 MeV/amu He/H will rise as confirmed in observations of large and/or hard proton events (Reames et al. [13]). *Energy dependence is important and one should not be surprised to see different temporal behavior of the abundance ratios at high and low energies.* For example, in the 2000 April 4 event with few ≥ 9 MeV but many ≥ 0.9 MeV protons, He/H falls at 2.2 MeV/amu (Ng et al. [14]) but rises 'anomalously' at 0.23 MeV/amu (Ho et al. [15], Fig. 3). Similarly, the model [3] predicts that initially Fe/O falls at high energy but *rises* at sufficiently *low* E/A for ample protons at $\geq 16E/A$ (see their Figs. 1 and 8). Indeed in the 1998 April 20 event, Fe/O falls at 2.6 MeV/amu (Fig. 3) but rises at 0.23 MeV/amu (Ho et al. [15], Fig. 4).

STREAMING LIMITED SEP ENERGY SPECTRA

SEP intensity energy spectra provide another means to study how self-generated waves throttle SEP transport. The descending energy spectra of shock-accelerated SEPs suggest that the streaming limit should extend to higher energy for larger event size. Figure 4a shows observations in five *strong* ground level events (GLEs) of *flattened* proton and O ion intensity spectra at $E < 5$ to 30 MeV and $E/A < 3$ to 5 MeV/amu, respectively[16]. These 'plateau' spectra are averaged in a time interval that includes slow particles and ends hours before shock arrival. Preliminary simultaneous model fits for both species are also shown [9]. Figure 4b contrasts the proton energy spectra of the weak 1998 May 2 GLE and the strong 2003 Oct 28 GLE. In the *weak* GLE, the intensity rises monotonically toward low energy, becoming comparable to or exceeding that in the strong GLE at $E < 1$ MeV ($P < 43$ MV). Also shown in Figure 4b are preliminary

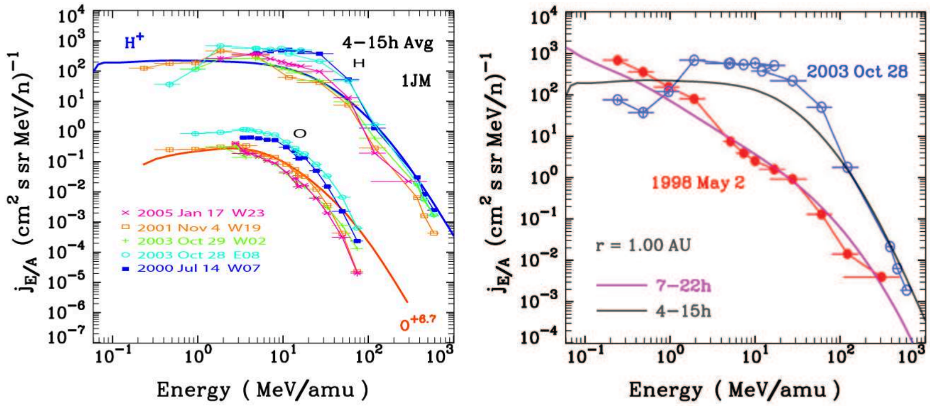

FIGURE 4. Observation (Reames and Ng [16]) and model prediction (Ng et al. [9]) of (a) 'plateau' H and O intensity spectra in five strong GLEs and (b) 'plateau' H spectra for a strong and a weak GLE.

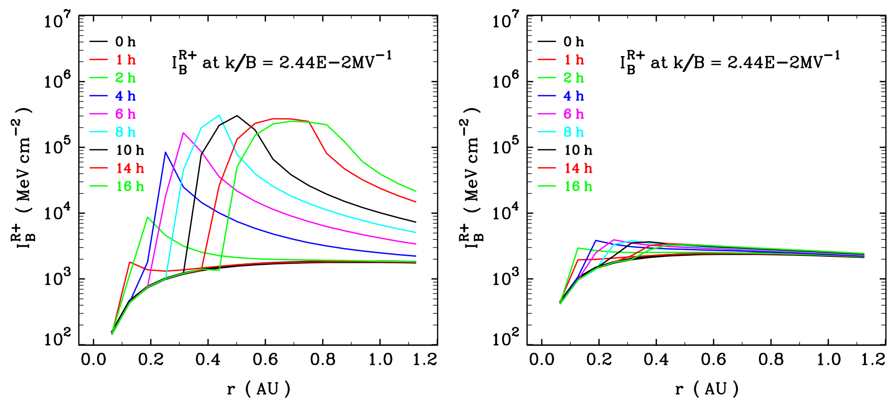

FIGURE 5. Evolving radial profile of I^{R+} wave intensity at $k/B = 0.0244$ MV^{-1} (resonant with 1 MeV protons at $\mu \sim 1$) in (a) 2003 Oct 28 strong GLE and (b) 1998 May 2 weak GLE (Ng et al. [9]).

model predictions calculated with weak and soft SEP injection for the weak GLE versus strong and hard SEP injection for the strong GLEs [9]. Further insight is provided by Figure 5 showing huge/little growth of I^{R+} wave intensity at $k/B = 0.0244$ MV^{-1} for the strong/weak GLE. Clearly, only strong GLEs have numerous enough > 1 MeV protons to hugely amplify waves to limit < 1 MeV SEP intensity and flatten the intensity spectra at low energy at 1 AU. Streaming limit thus complicates estimation of the total number and total energy of SEPs in an event from observation at 1 AU.

BOOTSTRAP CORONAL SHOCK ACCELERATION

Can a *finite-life* CME-driven coronal shock accelerate particles fast enough in typically low ambient wave intensities to agree with SEP observations? In the Ng and Reames [17] bootstrap shock acceleration model, protons are indeed accelerated to ~ 300 MeV in 10 minutes by a 2500 km/s parallel shock launched at 3.5 $r_\odot$, despite weak ambient

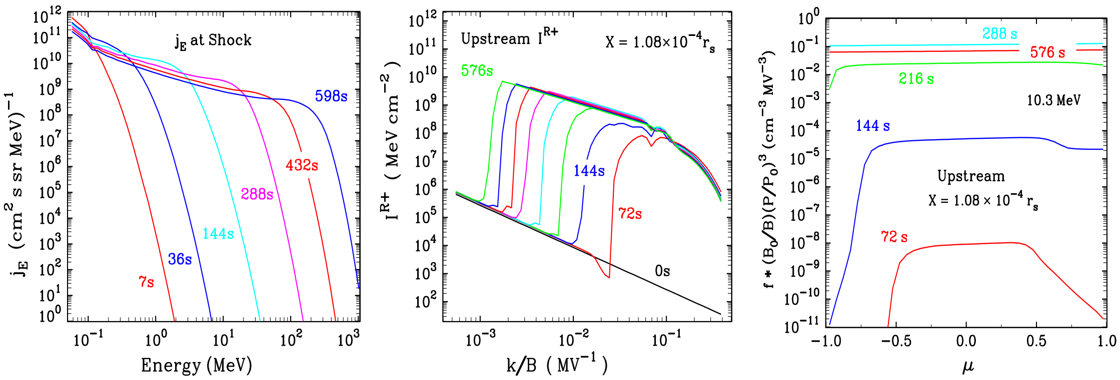

FIGURE 6. Evolution over 600 s of (a) proton j_E vs E, (b) I^{R+} wave intensity vs k/B, (c) proton phase-space density f vs μ at 10 MeV, just upstream of shock. (Ng and Reames [17])

waves. Here again, self-consistent amplification of Alfvén waves is the key.

Figures 6a,b show the coupled growth of the SEP and Alfvén wave spectra just upstream of the traveling shock, while Figure 6c gives a more intimate look at the evolution of the SEP phase-space density f versus μ at 10 MeV [17]. As f at 10 MeV grows by orders of magnitude, it fills out the μ-space (Fig. 6c) and simultaneously the 'knee' energy $E_{\rm knee}(t)$, where the j_E spectrum plunges, advances to > 10 MeV (Fig. 6a).

The streaming limit and bootstrap shock acceleration can be understood in *different spatial regions* via the resonance condition (1), which is satisfied for the same wavenumber k by (large P, small μ) and (small P, large μ) simultaneously. Thus, numerous upstream protons near the shock at $E < E_{\rm knee}$ and $\mu > 0.6$ excite waves which scatter $E \geq E_{\rm knee}$ protons at $\mu < 0.3$ to bootstrap their acceleration. For example, at $t \sim 200$ s, the acceleration becomes quasi-steady at 10 MeV, $E_{\rm knee}(t)$ advances to > 10 MeV and numerous 10 MeV protons fill out the μ-space near the shock. As the ≤ 10 MeV protons stream away from the shock they begin making upstream waves at $\mu > 0.6$ to advance shock acceleration to the next stage at $E \geq E_{\rm knee}(t) > 10$ MeV.

DISCISSION AND CONCLUSION

Wave amplification by streaming energetic charged particles is derived in e.g., Lee [18] and in [3, Appendix B] via energy conservation. SEP-amplified waves are studied or included in many other theoretical models, e.g., Vainio [19] and Li et al. [20]. ULF waves have been often observed with backstreaming < 100 keV protons upstream of the Earth's bow shock (e.g. Paschmann et al. [21], Eastwood et al. [22]) and less frequently at lower frequencies resonant with < 1 MeV protons at IP shocks (Tsurutani et al. [23], Vinãs et al. [24], Sanderson et al. [26], Bamert et al. [27]). However, direct evidence at 1 AU of > 1 MeV proton-amplified waves early in a SEP event has not been reported. The reason for this is three-fold. Shock acceleration efficiency generally decreases steeply with r, wave amplification decreases steeply from shock (compare I_B at $k/B = 0.0244$ MV^{-1}1 at 1 AU in Figure 5a and at $4r_\odot$ in Figure 6b), and Alfvén waves constitute only $\sim 10\%$ of ambient IP magnetic field (IMF) power spectrum. The wave intensities predicted at

1 AU by Ng et al. [3] (their Figs. 3 and 10) are below or comparable to the observed background IMF power spectrum (Leamon et al. [25]). Currently the best evidence for strong wave growth in the inner heliosphere comes indirectly from SEP observations. In the near future Solar Orbiter and Solar Probe Plus may observe the amplified waves in association with SEPs from their vantage points close to the Sun.

The many intriguing SEP behaviors - streaming-limited intensity, complex variation of elemental abundances with time, energy, and from event to event, as well as rapid shock acceleration despite weak ambient waves - all point to self-amplified waves as a common denominator. These behaviors are prevalent in *large* gradual events of space-weather significance. Successful modeling of these observed SEP characteristics requires self-consistent treatment of wave-particle resonant interaction with full μ, v, and A/Q-dependence. Continuing observation, analysis, and modeling of multi-species energetic ions in SEP events will allow us to better understand the physics of wave-particle interaction and their consequences - a prerequisite for space weather forecasting.

ACKNOWLEDGMENTS

Work by CKN, DVR, and AJT are supported in part by NASA grants NNX09AU98G, NNX08AQ02G, and NNH09AK79I, respectively.

REFERENCES

1. C. K. Ng and D. V. Reames, *Astrophys. J.*, **424**, 1032–1048 (1994).
2. D. V. Reames and C. K. Ng, *Astrophys. J.*, **504**, 1002–1005 (1998).
3. C. K. Ng, D. V. Reames and A. J. Tylka, *Astrophys. J.*, **591**, 461–485 (2003).
4. D. Lario, R. B. Decker and A. Aran, *AIP Conf. Proc.*, **1039**, 156–160 (2008).
5. M. A. Lee, *Mon. Not. R. Astron. Soc.*, **182**, 147–156 (1978).
6. M. A. Lee, *J. Geophys. Res.*, **88**, 6109–6119 (1983).
7. B. E. Gordon et al., *J. Geophys. Res.*, **104**, 28,263–28,277 (1999).
8. M. A. Lee, *Astrophys. J. Suppl. Ser.*, **158**, 38–67 (2005).
9. C. K. Ng, D. V. Reames and A. J. Tylka, *in prep* (2011).
10. A. J. Tylka, D. V. Reames and C. K. Ng, *Geophys. Res. Lett.*, **26**, 2141–2144 (1999).
11. C. K. Ng, D. V. Reames and A. J. Tylka, *Geophys. Res. Lett.*, **26**, 2145–2148 (1999).
12. A. J. Tylka, *J. Geophys. Res.*, **106**, 25333–25352 (2001).
13. D. V. Reames, C. K. Ng and A. J. Tylka, *Astrophys. J.*, **531**, L83-L86, (2000).
14. C. K. Ng, D. V. Reames and A. J. Tylka, *Proc. 27th ICRC (Hamburg)*, **8**, 3140–3143 (2001).
15. G. C. Ho et al., *Solar Wind 10, AIP Conf. Proc.*, **679**, 624–627 (2003)
16. D. V. Reames and C. K. Ng, *Astrophys. J.*, **723**, 1286–1293 (2010).
17. C. K. Ng and D. V. Reames, *Astrophys. J.*, **686**, L123–L126 (2008).
18. M. A. Lee, *Plasma Phys.*, **13**, 1079–1098 (1971).
19. R. Vanio, *Astron. Astrophys.*, **406**, 735–740 (2003).
20. G. Li, G. P. Zank and W. K. M. Rice, *J. Geophys. Res.*, **110**, A06104, doi:10.1029/2004JA010600 (2005).
21. Paschmann et al., *Geophys. Res. Lett.*, **6**, 209–212 (1979).
22. J. P. Eastwood et al., *Ann. Geophys.*, **21**, 1457–1465 (2003).
23. B. T. Tsurutani, E. J. Smith and D. E. Jones, *J. Geophys. Res.*, **88**, 5645–5656 (1983).
24. A. F. Vinãs, M. I. Goldstein and M. H. Acuña, *J. Geophys. Res.*, **89**, 3762–3774 (1984).
25. R. J. Leamon et al., *J. Geophys. Res.*, **103**, 4775–4787 (1998).
26. T. R. Sanderson et al., *J. Geophys. Res.*, **90**, 3973–3980 (1985).
27. T. R. Bamert et al., *Astrophys. J.*, **601**, L99–L102 (2004).